

Unusually high electrical conductivity of phlogopite: the possible role of fluorine and geophysical implications

Yan Li¹ · Xiaozhi Yang¹ · Jin-Hai Yu¹ · Yuan-Feng Cai¹

Received: 11 November 2015 / Accepted: 10 March 2016 / Published online: 30 March 2016
© Springer-Verlag Berlin Heidelberg 2016

Abstract Phlogopite is an accessory mineral often found in mantle samples from various tectonic settings of continental regions. Considerable effort has been expended on the effect of phlogopite on some key chemical and petrological processes of the upper mantle, such as the recycling of K, F and H₂O and the generation of K-rich fluids/melts; in contrast, less attention has been devoted to its physical properties. In this study, the orientation-related electrical conductivities of phlogopite single crystals have been experimentally determined at 1 GPa and 200–900 °C with an end-loaded piston cylinder press and a Solartron-1260 Impedance/Gain-Phase Analyzer in the frequency range of 10⁶–0.1 Hz. The results demonstrate that phlogopite can have unusually high conductivity, >0.01 S/m above ~600 °C and ~1 S/m at ~900 °C, significant electrical anisotropy, by a factor of >6 above ~900 °C, and large activation enthalpies, ~134–204 kJ/mol along different directions. The main charge carriers are probably K⁺ and F⁻, and fluorine may play a critical role in electrical conduction. The regional enrichment of K- and F-rich phlogopite, above subduction zones or in normal shields for example, could result in remarkable anomalies of electrical conductivity. This provides a new mechanism for explaining some

locally resolved electrical anomalies in the continental upper mantle.

Keywords Electrical conductivity · Single crystals · Phlogopite · Fluorine · Continental upper mantle · Experimental studies

Introduction

Phlogopite is an accessory mineral frequently observed in samples derived from the upper mantle, in particular from the subcontinental lithospheric mantle. It has been found in mantle-derived magmas such as kimberlite lavas and alkaline basalts and in mantle xenoliths captured by such magmas (e.g., Aoki 1975; Edwards et al. 1992; Fritschle et al. 2013). The presence of phlogopite in the upper mantle is widely considered the result of mantle metasomatism, e.g., by reactions between peridotites and ascending melts or fluids in the cratonic mantle and by interactions between peridotites and slab-dehydrated fluids in the mantle wedge of subduction zones (e.g., Menzies et al. 1987; Foley 1992; Zanetti et al. 1999; Shaw et al. 2005; Frost 2006; Luth 2014). Although volumetrically insignificant on the global scale when compared to olivine and pyroxenes, phlogopite can be of appreciable amounts, by volume on percent levels for example (e.g., Aoki 1975; Shaw et al. 2005), in some regional zones, and acts as an important repository of K, F and H₂O in the upper mantle down to >200 km depth (e.g., Konzett and Ulmer 1999; Frost 2006).

In the past decades, considerable effort by experimental studies has been expended on the crystal structure and stability field of phlogopite (e.g., Yoder and Eugster 1954; Hazen and Finger 1978; Konzett and Ulmer 1999; Trønnes 2002; Frost 2006), and the importance of phlogopite in

Communicated by Jochen Hoefs.

Electronic supplementary material The online version of this article (doi:10.1007/s00410-016-1252-x) contains supplementary material, which is available to authorized users.

✉ Xiaozhi Yang
xzyang@nju.edu.cn

¹ State Key Laboratory for Mineral Deposits Research, School of Earth Sciences and Engineering, Nanjing University, Nanjing 210023, People's Republic of China

affecting some key chemical and petrological processes of the upper mantle, including the recycling of K, F and H₂O (e.g., Schmidt 1996; Frost 2006), the incompatible trace-element composition (e.g., LaTourrette et al. 1995; Konzett et al. 2012), the effect on partial melting (e.g., Mysen and Boettcher 1975; Sudo and Tatsumi 1990) and the generation of K-rich melts or fluids (e.g., Foley 1993; Condamine and Medard 2014). In contrast, less attention has been paid to the physical behaviors of phlogopite at high pressure and temperature and its influence on mantle properties.

In this study, we have experimentally determined the orientation-related electrical conductivity of single-crystal phlogopite at 1 GPa and 200–900 °C, with two natural phlogopite single crystals as the starting material. The results show that phlogopite can have unusually high conductivity and significant electrical anisotropy at upper mantle conditions, and are potentially of crucial implications for a better knowledge of the electrical structure in some regional zones of the continental upper mantle.

Experimental and analytical methods

The starting materials were two gem-quality, tabular and pseudo-hexagonally shaped phlogopite single crystals, ~10 × 8 × 7 mm in dimension from unknown locality (Ph11) and ~25 × 25 × 20 mm in dimension from Mogok, Burma (Ph12). These samples were selected from >20 natural phlogopites from different localities: One of our initial attempts was to measure the electrical conductivity of a series of phlogopite crystals with a systematic variation in composition (especially for K and F), but this was not very successful due to the difficulty in obtaining samples of suitable size, good quality and appropriate composition. The crystals are chemically homogeneous for each, as determined by multi-point electron microprobe analyses, and their compositions are similar except for K and F, which each differs by ~0.5 wt% (Table 1). The K and F contents of these samples are intermediate in mantle phlogopites

from the world (Supplementary Fig. S1). H₂O contents of the samples are, respectively, ~0.3 and 0.5 wt%, determined by Fourier transform infrared (FTIR) spectroscopy (see below). Cylindrical cores with a diameter of ~3.0 mm and a length of ~1.8 mm were prepared along three nearly perpendicular directions, labeled as ⊥(001), ⊥(010) and ⊥(110), respectively (Supplementary Fig. S2).

Water contents of the samples before and after electrical conductivity measurements were determined from the polarized FTIR spectra along three mutually perpendicular directions, following the method of Libowitzky and Rossman (1996). IR spectra were recorded with a Bruker Vertex 70V FTIR spectrometer coupled with a Hyperion 2000 IR microscope. 128 scans were accumulated for each spectrum with an aperture size of 60 × 60 μm, a resolution of 4 cm⁻¹, a globar source, a KBr/Ge beam splitter and an mid-band MCT detector. A ZnSe wire-grid polarizer was used for polarized radiation, and polarized spectra were acquired with the electric field vector (*E*) parallel to three orthogonal directions. Optically clean areas free of inclusions or cracks were chosen for the analyses. During the measurements, the optics of the spectrometer were kept under vacuum, and the optics of the microscope were continuously purged by H₂O- and CO₂-free, purified air. Water content was calculated from the total absorbance of OH in the wave number 3800–3000 cm⁻¹, by summing the thickness-normalized integral absorbance along the three directions and using the mineral-specific integral absorption coefficient of phlogopite from Rouxhet (1970). Given the reliability of the calibration coefficient, the uncertainty of H₂O concentration is ≤10 %, owing mainly to baseline corrections.

Earth materials usually exhibit semi-conductive behavior at elevated conditions. The relative importance of impedance spectroscopy by sweeping over a wide range of frequencies, rather than by determinations at a single frequency or by direct current (DC) method which may introduce significant non-systematic uncertainty, in characterizing the electrical conductivity of silicate materials at high temperatures has

Table 1 Chemical composition of the starting and recovered samples (wt%)

	SiO ₂	TiO ₂	Al ₂ O ₃	Cr ₂ O ₃	FeO	MnO	MgO	CaO	Na ₂ O	K ₂ O	NiO	F	Cl	H ₂ O	Total
<i>Starting materials</i>															
Ph11	41.54	0.06	17.35	0.07	0.11	0.02	25.63	<0.01	0.15	9.99	<0.01	2.31	0.00	0.31	97.53
Ph12	41.90	0.32	16.99	0.04	0.16	0.02	25.88	<0.01	0.07	10.46	0.01	2.75	0.01	0.45	99.03
<i>Recovered materials</i>															
Ph11 ⊥(010)	42.53	0.08	16.75	0.04	0.10	0.02	25.66	0.01	0.20	9.84	<0.01	2.29	0.04	0.30	97.87
Ph12 ⊥(010)	41.75	0.26	17.07	0.02	0.20	<0.01	26.03	<0.01	0.06	10.42	<0.01	2.77	0.02	0.46	99.05
Ph12 ⊥(110)	41.72	0.27	17.11	0.01	0.19	<0.01	26.11	<0.01	0.05	10.54	<0.01	2.70	<0.01	0.49	99.19
Ph12 ⊥(001)	41.93	0.33	17.23	0.07	0.15	<0.01	26.99	<0.01	0.08	10.22	0.04	2.77	<0.01	0.50	100.30

Assuming all Fe as FeO. Trace elements were not measured (note that some natural phlogopite may contain abundant BaO, up to ~1–2 wt%)

been well documented in many available publications (e.g., Huebner and Dillenburg 1995; Barsoukov and Macdonald 2005). Complex impedance spectra of the samples were measured at 1 GPa and 200–900 °C using an end-loaded piston cylinder apparatus and a Solartron 1260 Impedance/Gain-Phase Analyzer, with a voltage of 500 mV and a frequency range of 10^6 –0.1 Hz in the standalone mode. The assembly setup is illustrated in Fig. 1, the same as that used in our previous work (Yang et al. 2011, 2012; Yang 2012; Yang and Heidelberg 2012; Yang and McCammon 2012). The sample, enclosed by hexagonal boron nitride (BN), was placed in a Pt capsule, with Pt disks as electrodes and Ni–NiO pairs as oxygen buffer for simulating the relatively oxidizing conditions in the shallow mantle. The capsule, sealed at its one end by soft BN and the other end by arc-welding, maintains the sample geometry and produces a rather closed system for the sample (upon gradual hot pressing), because of the low permeability and low strength of BN. The Pt–BN capsule design is crucial for controlling oxygen fugacity imposed on sample and for avoiding diffusion of graphite (heater) into sample. A piece of thin Ni foil connected to ground was placed between the graphite heater and the capsule to minimize possible leakage currents, and an S-type thermocouple was used to measure the temperature. No glue or cement was used to immobilize the experimental parts during assembly to avoid the release of volatiles upon heating. By this method, sample resistance on the order of up to $10^8 \Omega$ can be analyzed accurately, and oxygen fugacity inside the capsule and sample $\text{Fe}^{2+}/\text{Fe}^{3+}$ ratios can be controlled well during conductivity measurements (Yang et al. 2011, 2012).

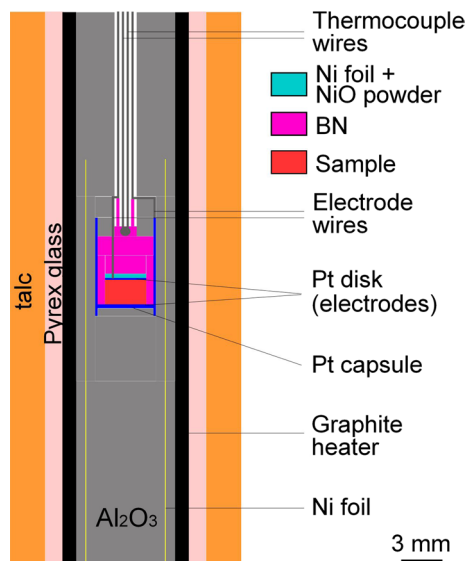


Fig. 1 Sample assembly for electrical conductivity measurements at high pressure and temperature

After the assembly was completed, it was heated in a furnace at ~ 125 °C overnight, and after loading into the piston cylinder press and reaching the designated pressure, the sample was heated again at ~ 200 °C for ~ 1 – 3 h (and for various durations in the first heating cycle up to ~ 500 – 600 °C). Under a constant pressure, temperature was raised at a rate of ~ 50 °C/min to the pre-set value, and the impedance spectroscopy analyses were made at various temperatures during subsequent heating and cooling cycles. After each run, the recovered capsule was polished for optical, backscatter and FTIR examinations. No other phases were detected in the samples, Ni–NiO pairs were still present, and distortions of sample geometry were negligible, although the absolute diameter and length decreased slightly (Fig. 2). The sample dimensions after the experiment, considering the effective contact between the sample and electrodes, were used to calculate the electrical conductivity (σ) by fitting the high-frequency impedance arc of the complex spectra according to $\sigma = L/S \times (1/R)$, where L and S are the sample length and cross-sectional area, respectively, and R is the resistance. During each measurement, the fluctuation of temperature was usually within ± 1 °C. The total uncertainty of temperature, including that arising from thermal gradient along the length of the capsule and from the thermocouple itself, is <20 °C, and the total uncertainty of the calculated conductivity, including sample dimensions and impedance arc fitting, is mostly $<10\%$ (Yang et al. 2011, 2012; Yang 2012; Yang and Heidelberg 2012; Yang and McCammon 2012).

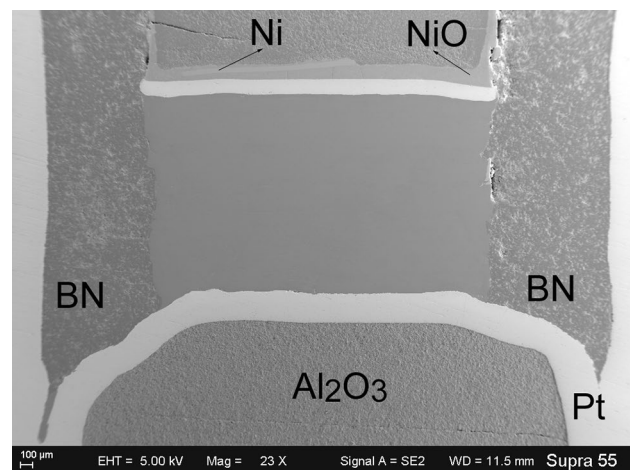


Fig. 2 Representative back-scatter image of recovered sample Ph11 \perp (001). Dark and light colors observed on the BN were due to non flat surface related to polishing. Small bright area at the sample–BN interface was a small piece of Ni (for controlling oxygen fugacity) introduced during assembling experimental parts

Results

The recovered samples demonstrated no zoned OH absorbance along core-to-rim paths, and the composition prior to and after the conductivity analyses was essentially the same given the analytical uncertainty (Table 1 and Supplementary Fig. S3), indicating that no significant sample dehydration or volatile loss occurred during the experiments. Representative impedance spectra are illustrated in Fig. 3. Usually the spectra show an arc through the whole frequency range at low temperatures and a high-frequency arc plus a low-frequency short tail at high temperatures.

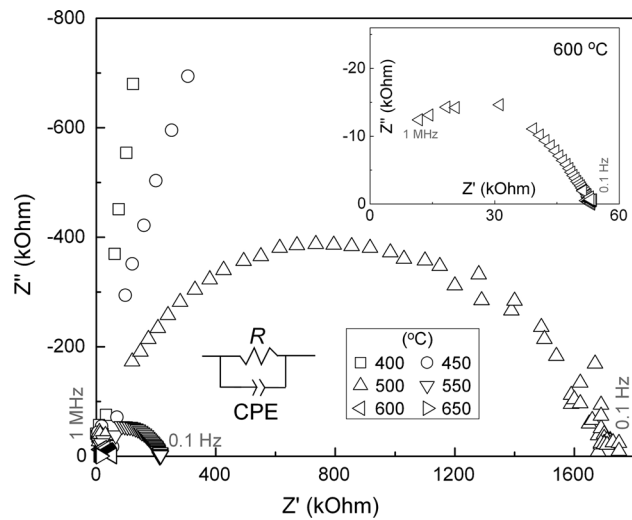
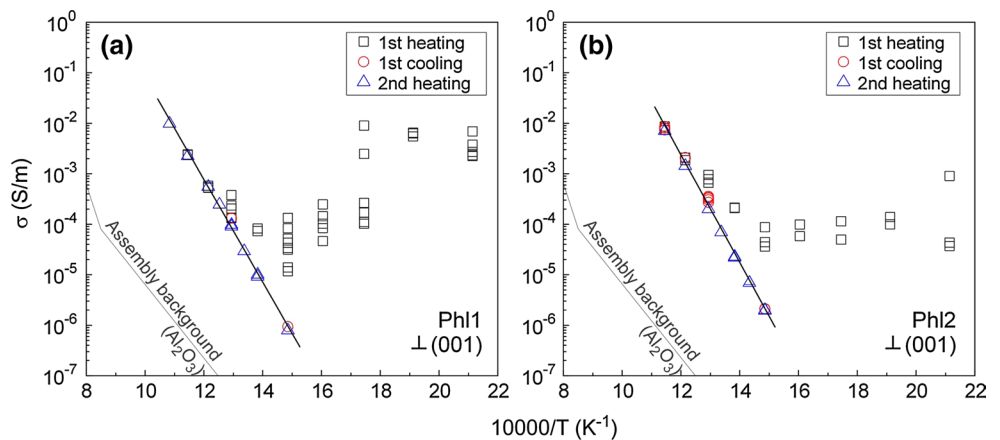


Fig. 3 Representative complex spectra of sample Phl2 $\perp(010)$. Z' and Z'' are the real and imaginary parts of the complex impedance, respectively. An equivalent circuit of a single R - CPE circuit element, a resistor R and a capacitor (CPE) in parallel, was used to fit the high-frequency arc, and the short tail in the low frequency range and the offset from the origin were not included. *Inset* shows the spectra at 600 °C. Some abnormal data points strongly deviating from the flat spectra were discarded

Fig. 4 Electrical conductivity measurement during the first heating cycle and comparison with subsequent cycles. **a** Sample Phl1 $\perp(001)$; **b** sample Phl2 $\perp(001)$. *Thick dark lines* are the linear fittings to the data from post-first heating cycles; *thin gray lines* are the assembly background conductivity by replacing the sample with a piece of dense ceramic Al_2O_3 (Yang et al. 2011), which increases rapidly above ~ 950 °C



The arc in the high frequency range is considered to be caused by sample interior conduction, and the tail in the low-frequency zone is usually attributed to electrode effects (Huebner and Dillenburg 1995; Yoshino 2010; Yang 2011; and references therein).

Electrical conductivity (σ) of silicate minerals as a function of temperature is usually expressed in the Arrhenius form:

$$\sigma = A_0 \cdot \exp\left(-\frac{\Delta H}{R \cdot T}\right) \tag{1}$$

where A_0 and ΔH are the pre-exponential factor and activation enthalpy (J/mol), respectively, R is the gas constant, and T is absolute temperature. During the first heating cycle of the conductivity measurements, the determined values at low temperatures show high data scatter, not following the Arrhenius relation, and deviate strongly from the trend at high temperatures and in the subsequent cycles (Fig. 4). This was caused by some remaining moisture in the system, which was gradually driven out upon heating, and the affected data were excluded from the analyses. Parameters from fitting the Arrhenius equation to the data are summarized in Table 2, and the measured data from different cooling/heating cycles and their fittings are demonstrated in Figs. 5 and 6. The yielded A_0 and ΔH are linearly related (Supplementary Fig. S4), suggesting that the conduction process follows the Meyer–Neldel rule (Jones 2014a). For each sample, the conductivities are reproducible between different cycles, suggesting the absence of system hysteresis. The activation enthalpies are ~ 134 – 204 kJ/mol, and the electrical conductivity is >0.01 S/m above ~ 600 °C and is ~ 1 S/m at ~ 900 °C. Along the direction $\perp(001)$, the electrical conductivity of Phl1 is slightly lower than that of Phl2, although their activation enthalpies are similar, ~ 200 kJ/mol. The results show significant anisotropy in the electrical conductivity: The conductivity along the direction $\perp(110)$ is higher than the other two directions at low temperatures but lower at high temperatures, where the

Table 2 Summary of samples and fitting parameters

	Orientation	L/S (m^{-1})	$\text{Log}_{10}A_0$ (S/m)	ΔH (kJ/mol)
Ph11	$\perp(001)$	256	9.06 ± 0.26	194 ± 4
Ph12	$\perp(001)$	245	10.15 ± 0.22	204 ± 3
	$\perp(010)$	263	8.41 ± 0.24	179 ± 4
	$\perp(110)$	210	6.09 ± 0.34	134 ± 5
	GM		8.22	172

L/S is the effective ratio of length to cross-sectional area of the recovered samples

Equation (1) was used to obtain the fitting parameters (uncertainty is 1 standard deviation)

GM is the geometrical mean of the electrical conductivity along three directions (see text)

direction $\perp(001)$ is the highest, and the difference can be a factor of >10 depending on temperature (Fig. 6). The bulk conductivity of the sample Ph12 is approximated by the geometrical mean (σ_{GM}) of the conductivity along the three directions by assuming a self-buffered isotropic medium (Shankland and Duba 1990),

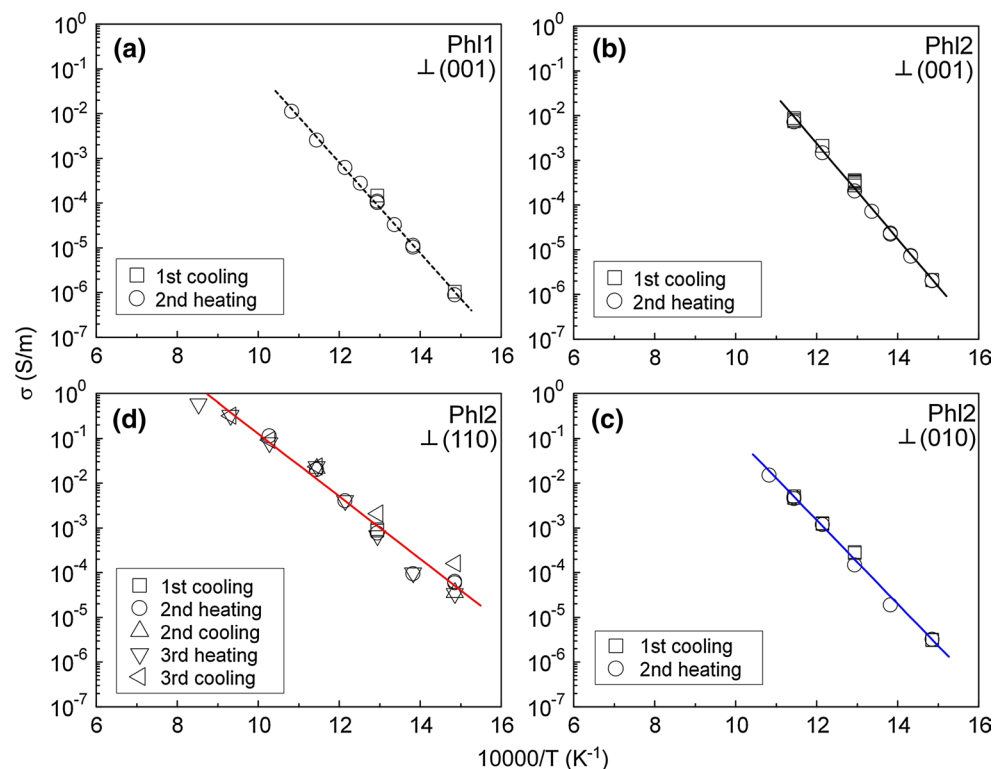
$$\sigma_{GM} = (\sigma_{\perp(001)} \cdot \sigma_{\perp(010)} \cdot \sigma_{\perp(110)})^{1/3} \quad (2)$$

and the modeled results are given in Table 2 and Fig. 6.

Comparison with other minerals and conduction mechanism

The electrical conductivities of some nominally hydrous minerals, such as serpentine (e.g., antigorite), pyrophyllite, lizardite and brucite, have been reported previously (Guo et al. 2011; Reynard et al. 2011; and references therein), and they differ profoundly from the results of this study for phlogopite (Fig. 6). In comparison with the phlogopite samples, the conductivities are larger for lizardite and brucite at low temperatures, e.g., below ~ 500 °C, but much smaller for serpentine and pyrophyllite, especially above ~ 450 °C, and the activation enthalpies of these minerals are in most cases ~ 80 – 115 kJ/mol, noticeably lower than those of the phlogopites, ~ 134 – 204 kJ/mol for different directions and 172 kJ/mol for the geometrical mean modeling (Table 2). Guseinov et al. (2005) have also determined the electrical properties of phlogopite; however, their reported electrical conductivity and activation enthalpies differ greatly from ours (Fig. 6). This may be accounted for by the measurements of Guseinov et al. (2005) on powdered samples, in vacuum (0.1 Pa) and particularly by using a DC method. The electrical conductivities of the Ph11 and Ph12, whether along individual directions or the modeled geometrical mean, are markedly larger, e.g., by orders of

Fig. 5 Electrical conductivity of single-crystal phlogopite **a** Ph11 $\perp(001)$, **b** Ph12 $\perp(001)$, **c** Ph12 $\perp(010)$ and **d** Ph12 $\perp(110)$. Lines are from least-squares regression of all the data in each panel



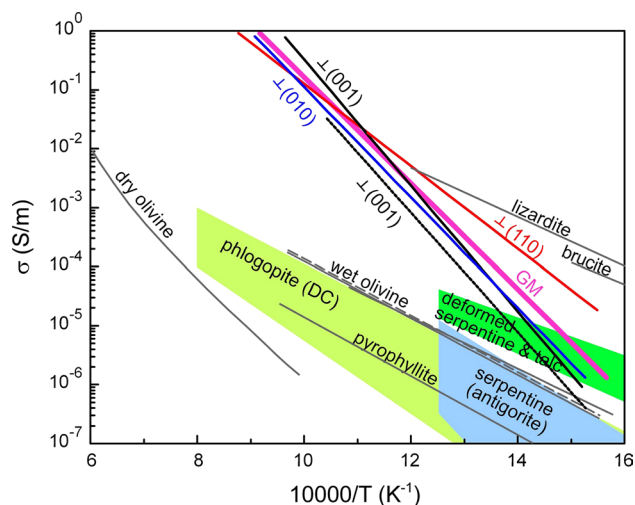


Fig. 6 Electrical conductivity of phlogopite and comparison with available reports. The *lines* for the single-crystal phlogopites are the same as shown in Fig. 5a–d, with slight extrapolation to higher temperature for samples Ph12 $\perp(001)$ and Ph12 $\perp(010)$. The *thick line*, labeled as GM, is the modeled geometrical mean (see text). Data sources for nominally hydrous phases: phlogopite (DC) (Guseinov et al. 2005), deformed serpentine and talc (Guo et al. 2011), serpentine, pyrophyllite, lizardite and brucite (Reynard et al. 2011; and references therein); data sources for nominally anhydrous olivine: dry (SEO3; Constable 2006)—modeled data under QFM buffer at ambient pressure, and wet (with 40 ppm H₂O; Yang 2012)—measured data under Ni–NiO buffer at 1 GPa for single crystals along [001], [010] and [100] directions

magnitude above ~ 400 °C (Fig. 6), than those of nominally anhydrous olivine, either the modeled values of dry olivine with oxygen fugacity buffered by quartz–fayalite–magnetite (QFM) at ambient pressure (the SEO3 model; Constable 2006) or the measured data of wet olivine single crystals, with ~ 40 ppm H₂O, at upper mantle conditions (Yang 2012; See also discussion below about the conductivity of H-bearing olivine).

The presence of H, even on trace levels of tens to hundreds of ppm H₂O, greatly enhances the electrical conductivity of nominally anhydrous minerals, due to proton conduction (e.g., Huang et al. 2005; Wang et al. 2006; Yoshino et al. 2006, 2009; Dai and Karato 2009; Poe et al. 2010; Yang et al. 2011, 2012; Yang 2012; Yang and McCammon 2012). As a result, the measured high conductivity of phlogopites may, at first sight, be well attributed to their high H₂O contents, ~ 0.3 and 0.5 wt%. This is, however, not supported by considering the reasons below: (1) with H as the main charge carrier, the activation enthalpies of nominally anhydrous minerals are mostly less than ~ 100 kJ/mol; (2) for nominally hydrous minerals with a few percent H₂O (by weight), the conductivity could be ~ 100 – $10,000$ times lower at similar higher temperatures, e.g., for serpentine, talc and pyrophyllite (Fig. 6), ruling out a significant and

general role of H in promoting conductivity, and in case of high conductivity where H-conduction may be important, e.g., for lizardite and brucite (Fig. 6), the activation enthalpies are only ~ 80 kJ/mol [note that the reported activation enthalpies of nominally hydrous minerals due to conduction by H, whatever their conductivities, are in most cases < 90 kJ/mol (e.g., Guo et al. 2011; Reynard et al. 2011)]. Conduction by small polarons, e.g., hopping of electron holes between Fe²⁺ and Fe³⁺, is considered the main mechanism of charge transport in Fe-bearing dry nominally anhydrous minerals (e.g., Dai and Karato 2009; Yoshino et al. 2009; Yang et al. 2011, 2012; Yang and Heidelbach 2012; Yang and McCammon 2012) and also in Fe-containing nominally hydrous minerals such as serpentine and pyrophyllite (Reynard et al. 2011), but is unlikely the dominant mechanism in the phlogopite samples, because of their very low bulk Fe contents, ~ 0.10 – 0.20 wt% for total FeO (Table 1).

The high electrical conductivity and large activation enthalpy of the phlogopites thus appear unique among nominally hydrous minerals and suggest that conduction is controlled by the migration of other ions. The most promising candidates are K and F, due to their significant amounts in the samples (Table 1) and high mobility at elevated conditions in silicate materials (Zhang and Cherniak 2010). In particular, it has been demonstrated by experimental studies that the presence of F promotes the alkali interdiffusion rate by 4 orders of magnitude at 600–800 °C in feldspar (Snow and Kidman 1991), and can enhance profoundly the rate of cation diffusion in melts (Johnston et al. 1974). Assuming a similar effect of F on the diffusivity of K in phlogopite, it would be not surprising that the electrical conductivity could be very high as measured here. Moreover, the ideal H₂O concentration of phlogopite is ~ 4 wt%, although mantle phlogopites range in OH content to values both significantly lower and slightly higher (Frost 2006), and the ~ 0.3 – 0.5 wt% H₂O in our samples may therefore indicate abundant sites of vacant OH[−]. This would facilitate the transfer of F[−] in the crystal lattice at high temperatures, because of the similar ionic charge and radius between F[−] and OH[−] (Shannon 1976), and thus influence electrical conductivity. Accepting this, the measured slightly lower conductivity of the Ph11 relative to Ph12 (Fig. 6), along the direction $\perp(001)$, may be well accounted for by their difference in both K₂O and F contents, by ~ 0.5 wt% for each (Table 1). Unfortunately, a robust conclusion about the quantitative effect of K₂O and F on the conductivity of phlogopite, based only on the data of the current two samples, is not possible, and because no diffusion data have been reported for K and F in phlogopite, attempts for modeling sample conductivity using their diffusivity, e.g., through the Nernst–Einstein equation, and for a comparison with the measured data, appear not likely.

Further studies on the conductivity of gem-quality phlogopites with a systematic variation in K and F abundance and/or on the diffusion of K and F in phlogopite are necessary.

In the past decades, extensive studies have been conducted on measuring the electrical conductivity of various mantle and crustal minerals, and the electrical conduction has been nearly exclusively attributed to the migration of one or several of the following charge carriers: oxygen vacancies, protons, small polarons and other cations such as Mg^{2+} , although it should be noted that conduction by the last species may only be observed at extremely high temperatures (e.g., Xu and Shankland 1999; Xu et al. 2000; Huang et al. 2005; Romano et al. 2006; Wang et al. 2006; Yoshino et al. 2006, 2009; Dai and Karato 2009; Poe et al. 2010; Yoshino 2010; Guo et al. 2011; Reynard et al. 2011; Yang et al. 2011, 2012; Yang 2012; Yang and McCammon 2012). It follows that, if the discussions above, about the conduction mechanism of phlogopite, are acceptable, the role of fluorine and its effect on the mobility of other ions would also be important in the electrical conduction of Earth materials at elevated conditions, which has never received any attention (to our knowledge, this work is the first report on this topic, although rather preliminary). It appears that the main constitutive minerals of the mantle commonly contain trace amounts of F, e.g., with an abundance of a few to tens of ppm for pyroxenes and olivine (Beyer et al. 2012; Mosenfelder and Rossman 2013a, b), and that the solubility of F can be thousands of ppm in pyroxenes, olivine, wadsleyite and ringwoodite, likely with a similar incorporation mechanism as OH (e.g., Beyer et al. 2012; Roberge et al. 2015). We thus suggest that the influence of F on the conductivity of mantle minerals should be considered.

Implications for regional electrical anomalies in continental upper mantle

The effect of pressure, for a variation of a few GPa in the shallow mantle, and of grain size, for a dimension above $\sim 5 \mu m$ which is typical in the upper mantle, on the electrical conductivity of silicate minerals is negligible compared to temperature and chemical composition (e.g., Xu et al. 2000; Yang and Heidelberg 2012). This can be applied to regions where fluids or melts are absent, e.g., for most of the mantle. Also, it has been experimentally demonstrated that conduction by oxygen vacancies or small polarons continues up to $\sim 1400 \text{ }^\circ\text{C}$ (to even higher) and by protons up to $\sim 1100 \text{ }^\circ\text{C}$ (before apparent dehydration) for nominally anhydrous minerals (Xu et al. 2000; Romano et al. 2006; Yang and McCammon 2012); we thus assume that our measured data, for conduction dominated probably by F and K, can be extrapolated to reasonably

higher temperatures, e.g., $1000\text{--}1200 \text{ }^\circ\text{C}$, on the basis of the yielded parameters (Table 2), even though our measurements were taken up to $900 \text{ }^\circ\text{C}$ and our assembly in Fig. 1 was not able to work well above $\sim 1000 \text{ }^\circ\text{C}$ (Yang et al. 2011). This kind of data extrapolation has been commonly used in many available studies, due to technical difficulties in conductivity experiments (e.g., Huang et al. 2005; Romano et al. 2006; Wang et al. 2006; Yoshino et al. 2006, 2009; Dai and Karato 2009; Poe et al. 2010; Yang et al. 2011, 2012; Yang 2012; Yang and McCammon 2012). Accordingly, the electrical conductivity of phlogopite under upper mantle conditions can be estimated. Considering the data of sample Ph12, the calculated conductivity is $\sim 4\text{--}61$ and $22\text{--}837 \text{ S/m}$ for the different directions and ~ 14 and 128 S/m for the modeled geometrical mean at 1000 and $1200 \text{ }^\circ\text{C}$, respectively.

As mentioned before and documented elsewhere, phlogopite is a major repository of K and F in the upper mantle down to $>200 \text{ km}$ depth, and its stability field is up to $\sim 9 \text{ GPa}$ at $\sim 1000 \text{ }^\circ\text{C}$ and to $\sim 1250 \text{ }^\circ\text{C}$ at $\sim 3\text{--}7 \text{ GPa}$, with stability conditions beyond many other common hydrous phases (e.g., Yoder and Eugster 1954; Konzett and Ulmer 1999; Trønnes 2002; Frost 2006; Konzett et al. 2012). In natural phlogopites of mantle origin, the F contents range mostly from 0 to $\sim 5 \text{ wt\%}$, although greater values up to $\sim 8\text{--}9.5 \text{ wt\%}$ have also been reported, and the K_2O contents are mostly $\sim 8\text{--}11 \text{ wt\%}$ (Supplementary Fig. S1 and references therein). The very high electrical conductivity of the phlogopite with moderate K and F contents (Fig. S1), as calculated above, indicates that phlogopite is able to affect the electrical structure of regional zones in the continental upper mantle. For a quantitative evaluation of the possible role of phlogopite, as a minor component in a rock system, in influencing the bulk electrical conductivity, however, the volume abundance of phlogopite and geometry of the matrix must be first considered.

The amount of phlogopite in the upper mantle is hard to constrain. Available studies have shown that phlogopites in mantle samples, such as kimberlites and mantle xenoliths, could be by crystallization at the original site in the upper mantle (mantle phlogopite for simplicity) and by reaction with the host magmas, e.g., kimberlite-related melts, immediately prior to eruption or during their rapid upward transport (secondary phlogopite) (Aoki 1975; Shaw et al. 2005; Giuliani et al. 2016; and references therein). The modal composition of mantle phlogopite has been reported as <1 to 3% and sometimes reaches $\sim 12 \%$ in peridotite xenoliths from some localities, e.g., the Kimberley area, South Africa (Aoki 1975). During the transfer of mantle samples to the surface and/or their short residence at shallow depths, however, high temperature of the host magmas may have caused decomposition of mantle phlogopite in them (partly or wholly), by considering the stability of

phlogopite. This is supported by a recent study that some mantle phlogopite crystals in kimberlites show good evidence of resorption (Giuliani et al. 2016). If so, petrographic estimation of mantle samples would underestimate the abundance of mantle phlogopite in their source regions. On the other hand, potassic and ultra-potassic magmatism has been recognized worldwide, especially in post-collisional settings, and such magmatism is widely attributed to melting of phlogopite-bearing peridotite (Condamine and Medard 2014; and references therein); the results of Mysen and Boettcher (1975) demonstrated that the addition of by volume 1–2 % phlogopite to a peridotite does not increase the K_2O content of generated melts. Thus, the proportion of phlogopite in some areas should be appreciated; otherwise, K-rich melts of significant volumes would not have been produced. Taken together, the presence of phlogopite in regional zones of the continental upper mantle, e.g., with a modal fraction in percent levels, appears robust.

Two textural types of mantle phlogopite, with occurrence as isolated grains or veins, have been identified in mantle samples (Aoki 1975; Shaw et al. 2005; Giuliani et al. 2016; and references therein). Mantle phlogopite is commonly linked to metasomatic processes, by infiltration of fluids or melts, and as such, many recent models have it being contained in veins, as proposed by Foley (1992), rather than distributed in the mantle peridotite (e.g., Luth 2014). This raises an important question whether (and to what extent) the observed isolated feature of mantle phlogopite in mantle samples efficiently preserved their initial textures, in particular when the complexities on the stability of phlogopite as discussed above are taken into account. The conductivity of a phlogopite-bearing peridotite would be significantly enhanced only if the phlogopite is interconnected, but not in isolated forms. With respect to veins in mantle samples, phlogopite could be associated with clinopyroxene, amphibole and other metasomatic minerals (Foley 1992; Luth 2014; Giuliani et al. 2016; and references therein), and interestingly, connected networks have been reported for mantle phlogopite grains, e.g., in xenoliths from the West Eifel Volcanic Field, Germany (see Fig. 3d in Shaw et al. 2005). Therefore, the following model estimation is performed.

The conductivity of a peridotite mantle with some conductive phlogopite can be calculated by available mixing relations used to characterize the bulk property of mineral mixtures (Shankland and Duba 1990). The conductivity of a peridotite can be obtained by considering the contribution of its constitutive olivine, orthopyroxene and clinopyroxene of equilibrium composition in both major and minor elements. A control of composition is important, because it strongly affects the conductivity of a mineral. For peridotite minerals of equilibrium composition, their conductivity data are lacking. Available studies have, however,

shown that, for dry San Carlos olivine and orthopyroxene of approximate equilibrium in major elements (Xu and Shankland 1999; Xu et al. 2000), their conductivities are close, and that, for either dry or wet orthopyroxene and clinopyroxene of equilibrium composition (Yang et al. 2011, 2012), their conductivities are similar at comparable conditions above ~ 600 °C (Supplementary Fig. S5). Therefore, we can reasonably assume that, given equilibrium in composition, the conductivities of olivine, orthopyroxene and clinopyroxene resemble each other at similar conditions, and that the conductivity of a peridotite can be approximated by its dominant olivine. The composition of phlogopite is largely related to metasomatic melts or fluids, and we thus do not consider seriously its elemental equilibrium with olivine. The bulk conductivity of a peridotite with connected vein phlogopite can then be calculated from the conductivities of olivine, the most abundant phase, and phlogopite, the more conductive phase, and the volume fractions (f) of these two minerals by the parallel model (σ_p):

$$\sigma_p = f_{\text{olivine}} \cdot \sigma_{\text{olivine}} + f_{\text{phlogopite}} \cdot \sigma_{\text{phlogopite}} \quad (3)$$

and by the Hashin and Shtrikman upper bound ($\sigma_{\text{HS}+}$):

$$\sigma_{\text{HS}+} = \sigma_{\text{phlogopite}} + f_{\text{olivine}} \cdot [(\sigma_{\text{olivine}} - \sigma_{\text{phlogopite}})^{-1} + f_{\text{phlogopite}} / (3 \cdot \sigma_{\text{phlogopite}})]^{-1} \quad (4)$$

The reported conductivity of H-bearing olivine is of some debate, particularly at OH contents above ~ 100 ppm H_2O (e.g., Wang et al. 2006; Yoshino et al. 2006, 2009; Poe et al. 2010; Yang 2012). Some of these studies were subjected to serious technical problems, such as single frequency impedance measurements, unpolarized FTIR analyses, fluid inclusions/grain boundary water in samples and/or sample dehydration during the runs (Dai and Karato 2009; Yang 2012; Yang et al. 2012; Gardés et al. 2014; Jones 2014b, 2016). Therefore, some reported data should be treated with caution by fitting to any models, although it has been shown that, by considering uncertainty and applying data correction, they are mostly consistent (Gardés et al. 2014). The experiments of Yang (2012), appearing rather free of such technical issues, have been conducted on single-crystal olivines with ~ 40 ppm H_2O , broadly comparable to the OH contents of olivine in the shallow mantle as noted in that paper. Accordingly, the extrapolated conductivity data of Yang (2012), ~ 0.002 S/m at 1000 °C and 0.007 S/m at 1200 °C, are used for the modeling (note that adoption of these values does not change the general result), along with the geometrical mean of the Ph12. Figure 7 displays how the bulk conductivity evolves with the volume fraction of phlogopite at 1000 and 1200 °C, respectively (note that the modeling and illustration are only to emphasize the possible strong effect of phlogopite on the conductivity of a rock

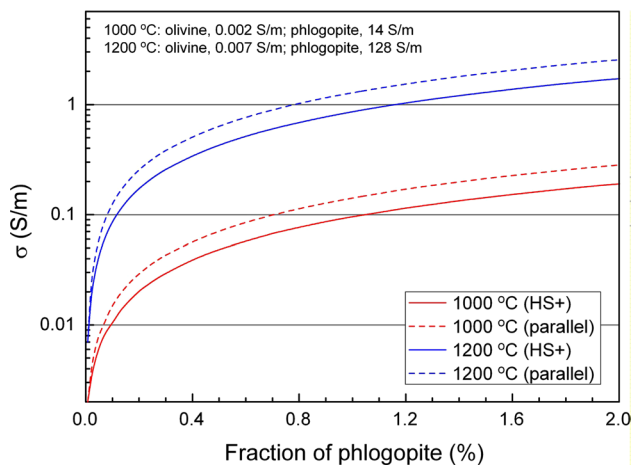


Fig. 7 Electrical conductivity of upper mantle by mixing peridotite and phlogopite at different volume fractions and temperatures. The Hashin and Shtrikman upper bound (HS+) and the parallel model were used for the modeling at 1000 and 1200 °C (see text). Electrical conductivity of peridotite was estimated from the dominant constituent olivine, by the data trend of hydrous olivine with ~40 ppm H₂O from Yang (2012) and Gardés et al. (2014), as illustrated in Fig. 5 to 1000 °C (~0.002 S/m) and 1200 °C (~0.007 S/m), and the highly conductive phlogopite, of which the electrical conductivity was calculated from the modeled geometrical mean of sample Ph12 (Fig. 6). The gray lines plotted at 0.01, 0.1 and 1 S/m are a guide for the eye

system, resembling the approaches in available reports for the role of fluids, melts or other grain boundary conductive phases, that complexities involving temperature and other factors are not considered, and that change of olivine conductivity, e.g., by slightly changing water content, does not change the general result). The results show that, with ~1 % phlogopite at 1000 and 1200 °C, the bulk conductivity reaches ~0.1 and 1 S/m, respectively. If the involved phlogopite is depleted in K and F and is thus of lower conductivity, as suggested by the discussion above, the modeled volume fractions would be higher.

As a result, the local presence of phlogopite in the continental upper mantle has the possibility to result in high electrical conductivity. Moreover, significant electrical anisotropy may have been produced by: (1) the spatial distribution of phlogopite as veins in peridotite, which can lead to different conductivities along directions, respectively, parallel and perpendicular to the veins (or phlogopite-rich layers), and/or (2) the alignment of phlogopite relative to shear stress, e.g., the difference of conductivity between the direction $\perp(001)$ and $\perp(110)$ is a factor of ~6 at 900 °C and ~40 at 1200 °C (Fig. 6, by data extrapolation), although no studies have been reported on the microstructure of vein-shape mantle phlogopite. In a previous report, Boerner et al. (1999) explained the resolved high conductivity of the shallow mantle beneath the southern Archean Churchill Province, western Canada, by the presence of

metasomatism-related phlogopite, under an assertion that phlogopite would be conductive because of an assumed role of its water (without any laboratory measurements). Our data lend support to their result; however, the conductive phlogopite is not caused by water but probably by F and K. This offers a new model for explaining some anomalous zones of high conductivity, ~0.01 to >0.1 S/m, and electrical anisotropy, by a factor of >2, in the continental shallow mantle (e.g., Jones 1999), since in these regions, the prevailing temperature may be only ~1000–1200 °C or lower, thus within the stability field of phlogopite.

This model, that F and K-rich phlogopite can produce electrical anomalies in the continental upper mantle, is similar to the one of Yang and McCammon (2012) that locally present Fe³⁺- and H-rich augite (and other pyroxenite analogues) may lead to zones of high electrical conductivity and significant electrical anisotropy in the deep continental lithosphere: Both are related to the macroscale petrological heterogeneity (solid rocks) of the upper mantle (Meibom and Anderson 2003). If so, geophysically resolved conductive zones in the continental upper mantle should not be always attributed to the presence of partial melts, saline fluids, graphite or sulfides (Jones 1999; Reynard et al. 2011; and references therein). This suggest that a single cause for the enhanced conductivity of the continental shallow mantle is unlikely, and that the complexity and diversity of mantle petrology must be considered for a clear picture of the fine structure and geophysical processes in the continental upper mantle.

Acknowledgments Discussions with Anton Beran helped to clarify issues on OH in phlogopite, and discussions with Andrea Giuliani helped to clarify issues on phlogopite in kimberlites. Wenlan Zhang assisted in electron microprobe analyses. Constructive comments by Alan Jones and four anonymous reviewers greatly improved the manuscript. This study was supported by Grants from the National Basic Research Program of China (973 project, 2014CB845904), the National Science Foundation of China (41590622 and 41372041), the Fundamental Research Funds for the Central Universities (PR China) and the Recruitment Program of Global Young Experts (PR China).

References

- Aoki K (1975) Origin of phlogopite and potassic richterite bearing peridotite xenoliths from South Africa. *Contrib Mineral Petrol* 53:145–156
- Barsoukov E, Macdonald JR (2005) Impedance spectroscopy theory, experiments and applications. John Wiley and Sons Inc, Hoboken
- Beyer C, Klemme S, Wiedenbeck M, Stracke A, Vollmer C (2012) Fluorine in nominally fluorine-free mantle minerals: experimental partitioning of F between olivine, orthopyroxene and silicate melts with implications for magmatic processes. *Earth Planet Sci Lett* 337–338:1–9
- Boerner DE, Kurtz RD, Craven JA, Ross GM, Jones FW, Davis WJ (1999) Electrical conductivity in the Precambrian lithosphere of western Canada. *Science* 283:668–670

- Condamine P, Medard E (2014) Experimental melting of phlogopite-bearing mantle at 1 GPa: implications for potassic magmatism. *Earth Planet Sci Lett* 397:80–92
- Constable S (2006) SEO3: a new model of olivine electrical conductivity. *Geophys J Int* 166:435–437
- Dai L, Karato SI (2009) Electrical conductivity of wadsleyite at high temperatures and high pressures. *Earth Planet Sci Lett* 287:277–283
- Edwards D, Rock NMS, Taylor WR, Griffin BJ, Ramsay RR (1992) Mineralogy and petrology of the Aries diamondiferous kimberlite pipe, central Kimberley Block, Western Australia. *J Petrol* 33:1157–1191
- Foley SF (1992) Vein-plus-wall-rock melting mechanisms in the lithosphere and the origin of potassic alkaline magmas. *Lithos* 28:435–453
- Foley SF (1993) An experimental study of olivine lamproite: first results from the diamond stability field. *Geochim Cosmochim Acta* 57:483–489
- Fritschle T, Prelević D, Foley SF, Jacob DE (2013) Petrological characterization of the mantle source of Mediterranean lamproites: indications from major and trace elements of phlogopite. *Chem Geol* 353:267–279
- Frost DJ (2006) The stability of hydrous mantle phases. *Rev Mineral Geochem* 62:243–271
- Gardés E, Gaillard F, Tarits P (2014) Toward a unified hydrous olivine electrical conductivity law. *Geochem Geophys Geosys* 15:4984–5000
- Giuliani A, Phillips D, Kamenetsky VS, Goemann K (2016) Constraints on kimberlite ascent mechanisms revealed by phlogopite compositions in kimberlites and mantle xenoliths. *Lithos* 240–243:190–201
- Guo X, Yoshino T, Katayama I (2011) Electrical conductivity anisotropy of deformed talc rocks and serpentinites at 3 GPa. *Phys Earth Planet Inter* 188:69–81
- Guseinov AA, Gargatsev IO, Gabitova RU (2005) Electrical conductivity of phlogopites at high temperatures. *Izv Phys Solid Earth* 41:670–679
- Hazen RM, Finger LW (1978) The crystal structure and compressibilities of layer minerals at high pressure. II. Phlogopite and chlorite. *Am Mineral* 63:293–296
- Huang X, Xu Y, Karato SI (2005) Water content in the transition zone from electrical conductivity of wadsleyite and ringwoodite. *Nature* 434:746–749
- Huebner JS, Dillenburg RG (1995) Impedance spectra of hot, dry silicate minerals and rock: qualitative interpretation of spectra. *Am Mineral* 80:46–64
- Johnston RF, Stark RA, Taylor J (1974) Diffusion in liquid slags. *Ironmak Steelmak* 1:220–227
- Jones AG (1999) Imaging the continental upper mantle using electromagnetic methods. *Lithos* 48:57–80
- Jones AG (2014a) Compensation of the Meyer–Neldel compensation law for H diffusion in minerals. *Geochem Geophys Geosys* 15:2616–2631
- Jones AG (2014b) Reconciling different equations for proton conduction using the Meyer–Neldel compensation rule. *Geochem Geophys Geosys*. doi:10.1002/2013GC004911
- Jones AG (2016) Proton conduction and hydrogen diffusion in olivine: an attempt to reconcile laboratory and field observations and implications for the role of grain boundary diffusion in enhancing conductivity. *Phys Chem Miner*. doi:10.1007/s00269-00015-00790-00265
- Konzett J, Ulmer P (1999) The stability of hydrous potassic phases in lherzolitic mantle—an experimental study to 9.5 GPa in simplified and natural bulk compositions. *J Petrol* 40:629–652
- Konzett J, Rhede D, Frost DJ (2012) The high PT stability of apatite and Cl partitioning between apatite and hydrous potassic phases in peridotite: an experimental study to 19 GPa with implications for the transport of P, Cl and K in the upper mantle. *Contrib Mineral Petrol* 163:277–296
- LaTourrette T, Hervig RL, Holloway JR (1995) Trace element partitioning between amphibole, phlogopite, and basanite melt. *Earth Planet Sci Lett* 135:13–30
- Libowitzky E, Rossman GR (1996) Principles of quantitative absorbance measurements in anisotropic crystals. *Phys Chem Miner* 23:319–327
- Luth RW (2014) Volatiles in Earth’s mantle. In: Holland HD, Turekian KK (eds) *Treatise on geochemistry*, 2nd edn. Elsevier, Amsterdam, pp 355–391
- Meibom A, Anderson DL (2003) The statistical upper mantle assemblage. *Earth Planet Sci Lett* 217:123–139
- Menzies MA, Rogers N, Tindle AG, Hawkesworth CJ (1987) Metasomatic and enrichment processes in lithospheric peridotites, an effect of asthenosphere-lithosphere interaction. In: Menzies MA, Hawkesworth CJ (eds) *Mantle metasomatism*. Academic Press, London, pp 313–361
- Mosenfelder JL, Rossman GR (2013a) Analysis of hydrogen and fluorine in pyroxenes: I. orthopyroxene. *Am Mineral* 98:1026–1041
- Mosenfelder JL, Rossman GR (2013b) Analysis of hydrogen and fluorine in pyroxenes: II. Clinopyroxene. *Am Mineral* 98:1042–1054
- Mysen BO, Boettcher AL (1975) Melting of a hydrous mantle: I. phase relations of natural peridotite at high pressures and temperatures with controlled activities of water, carbon dioxide, and hydrogen. *J Petrol* 16:520–548
- Poe BT, Romano C, Nestola F, Smyth JR (2010) Electrical conductivity anisotropy of dry and hydrous olivine at 8 GPa. *Phys Earth Planet Inter* 181:103–111
- Reynard B, Mibe K, Van de Moortele B (2011) Electrical conductivity of the serpentinised mantle and fluid flow in subduction zones. *Earth Planet Sci Lett* 307:387–394
- Roberge M, Bureau H, Bolfan-Casanova N, Frost DJ, Raepsaet C, Surble S, Khodja H, Auzende AL, Fiquet G (2015) Is the transition zone a deep reservoir for fluorine? *Earth Planet Sci Lett* 429:25–32
- Romano C, Poe BT, Kreidie N, McCammon C (2006) Electrical conductivities of pyrope-almandine garnets up to 19 GPa and 1700 °C. *Am Mineral* 91:1371–1377
- Rouxhet PG (1970) Hydroxyl stretching bands in micas: a quantitative interpretation. *Clay Miner* 8:375–388
- Schmidt MW (1996) Experimental constraints on recycling of potassium from subducted oceanic crust. *Science* 272:1927–1930
- Shankland TJ, Duba AG (1990) Standard electrical conductivity of isotropic, homogeneous olivine in the temperature range 1200–1500 °C. *Geophys J Int* 103:25–31
- Shannon RD (1976) Revised effective ionic radii and systematic studies of interatomic distances in halides and chalcogenides. *Acta Cryst A* 32:751–767
- Shaw CSJ, Eyzaguirre J, Fryer B, Gagnon J (2005) Regional variations in the mineralogy of metasomatic assemblages in mantle xenoliths from the West Eifel Volcanic Field, Germany. *J Petrol* 46:945–972
- Snow E, Kidman S (1991) Effect of fluorine on solid-state alkali interdiffusion rates in feldspar. *Nature* 349:231–233
- Sudo A, Tatsumi Y (1990) Phlogopite and K-amphibole in the upper mantle: implication for magma genesis in subduction zone. *Geophys Res Lett* 17:29–32
- Trønnes RG (2002) Stability range and decomposition of potassic richterite and phlogopite end members at 5–15 GPa. *Miner Petrol* 74:129–148
- Wang D, Mookherjee M, Xu Y, Karato S (2006) The effect of water on the electrical conductivity of olivine. *Nature* 443:977–980
- Xu Y, Shankland TJ (1999) Electrical conductivity of orthopyroxene and its high pressure phases. *Geophys Res Lett* 26:2645–2648

- Xu Y, Shankland TJ, Duba AG (2000) Pressure effect on electrical conductivity of mantle olivine. *Phys Earth Planet Inter* 118:149–161
- Yang X (2011) Origin of high electrical conductivity in the lower continental crust: a review. *Surv Geophys* 32:875–903
- Yang X (2012) Orientation-related electrical conductivity of hydrous olivine, clinopyroxene and plagioclase and implications for the structure of the lower continental crust and uppermost mantle. *Earth Planet Sci Lett* 317–318:241–250
- Yang X, Heidelbach F (2012) Grain size effect on the electrical conductivity of clinopyroxene. *Contrib Mineral Petrol* 163:939–947
- Yang X, McCammon C (2012) Fe³⁺-rich augite and high electrical conductivity in the deep lithosphere. *Geology* 40:131–134
- Yang X, Keppler H, McCammon C, Ni H, Xia Q, Fan Q (2011) The effect of water on the electrical conductivity of lower crustal clinopyroxene. *J Geophys Res* 116:B04208. doi:[10.1029/2010JB008010](https://doi.org/10.1029/2010JB008010)
- Yang X, Keppler H, McCammon C, Ni H (2012) Electrical conductivity of orthopyroxene and plagioclase in the lower crust. *Contrib Mineral Petrol* 163:33–48
- Yoder HS, Eugster HP (1954) Phlogopite synthesis and stability range. *Geochim Cosmochim Acta* 6:167–185
- Yoshino T (2010) Laboratory electrical conductivity measurement of mantle minerals. *Surv Geophys* 31:163–206
- Yoshino T, Matsuzaki T, Yamashita S, Katsura T (2006) Hydrous olivine unable to account for conductivity anomaly at the top of the asthenosphere. *Nature* 443:973–976
- Yoshino T, Matsuzaki T, Shatskiy A, Katsura T (2009) The effect of water on the electrical conductivity of olivine aggregates and its implications for the electrical structure of the upper mantle. *Earth Planet Sci Lett* 288:291–300
- Zanetti A, Mazzucchelli M, Rivalenti G, Vannucci R (1999) The Finero phlogopite-peridotite massif: an example of subduction-related metasomatism. *Contrib Mineral Petrol* 134:107–122
- Zhang Y, Cherniak DJ (2010) Diffusion in minerals and melts. *Mineralogical Society of America*, Chantilly, p 1036